FRACTIONAL ROBUST CONTROL WITH ISO-DAMPING PROPERTY

V. Pommier-Budinger*, Y. Janat*, D. Nelson-Gruel**, P. Lanusse** and A. Oustaloup**

*ISAE - 1, Place Blouin, 31056 Toulouse - France
fax: +33 (0)561 618 686 - e-mail: valerie.budinger@isae.fr
**LAPS UMR 5131 CNRS/Université Bordeaux I/ENSEIRB - 351, Cours de la Libération, 33405 Talence – France
fax: +33 (0)556 842 417 - e-mail: lanusse@ims-bordeaux.fr

Abstract:
This article deals with the problem of the reduction of structural vibrations with isodamping property. The proposed methodology is based on:
- a contour defined in the Nichols plane and significant of the damping ratio of the closed-loop response
- a robust control method that uses fractional order integration.

The methodology is applied to an aircraft wing model made with a beam and a tank whose different levels of fillings are considered as uncertainties.

Introduction

The reduction of structural vibration has been challenging engineers for many years. Innumerable applications exist where vibration control is beneficial, if not essential.
In the control of vibrations, the damping ratio is an important data since it indicates how quickly the vibrations decrease. When control of vibrations is at stake, it can be useful to control this parameter. Works have already been achieved to this end [1].

This article proposes a method in the frequency-domain to control uncertain plants while ensuring the damping ratio of the response. This method is based on the complex fractional order integration [2] that is used in two goals:
(i) the definition of a contour called “iso-damping” contour [3] whose graduation is the damping ratio in the Nichols plane,
(ii) the definition of an open-loop transfer function [5] whose part of the Nichols locus is an any-direction straight line segment that can tangent a Nichols contour or an iso-damping contour defined above.

The article falls into 4 parts. Section 1 introduces the transfer function of a complex non-integer integrator defining a generalized template which will be considered as part of an open-loop Nichols locus [5]. This transfer function is used in section 2 for the construction in the Nichols plane of a network of iso-damping contours [3,4].
Section 3 describes the CRONE (the French acronym of "Commande Robuste d'Ordre Non Entier") control based on complex fractional order differentiation [6]. This control methodology can be applied to SISO and MIMO plants and also plants with lightly damped modes. The interest of the fractional order is to define a transfer function with few parameters and thus to simplify design and optimization of the control system.
Section 4 presents an example of multivariable flexible structure which is an aircraft wing model made of a free-clamped beam with a water tank and co-localized piezoelectric ceramics used as actuators to limit the vibrations and as sensors to measure these vibrations. The different levels of filling of the tank make it possible to test the robustness of the damping ratio obtained with the CRONE control design associated to iso-damping contours.

I. Complex fractional integration

The transfer function of a real fractional or non-integer integrator of order n is given by [2]:

$$\beta(s)=\left(\frac{\omega_{cg}}{s}\right)^{n}, \quad n\in\mathrm{R}. \qquad (1)$$

The Nichols locus of a transfer function described by this integrator in a frequency interval $[\omega_A,\ \omega_B]$ is a vertical segment that will be called “vertical template” (Fig.1). The phase placement of this segment at the crossover frequency ω_{cg} depends on the order n and is worth $-n90°$.

From the extension of the description of the vertical template, the “generalized template” - that is to say an any-direction straight line segment in the Nichols plane - can be obtained using the complex non-integer integration of order n. $n = a + ib$ where the imaginary unit i of the integration order n is independent of the imaginary unit j of the variable s ($s=\sigma+\mathrm{j}\omega$). The transfer function of a complex non-integer integrator of order n is given by [1]:

$$\beta(s)=\left(\cosh\left(b\frac{\pi}{2}\right)\right)^{\mathrm{sign}(b)}\left(\frac{\omega_{cg}}{s}\right)^{a}\left(\mathrm{Re}_{/i}\left[\left(\frac{\omega_{cg}}{s}\right)^{ib}\right]\right)^{-\mathrm{sign}(b)}. \qquad (2)$$

The real part a defines the phase placement of the generalized template at ω_{cg}, $-\mathrm{Re}(n)90°$, and the imaginary part b defines its angle to the vertical (Fig.1).

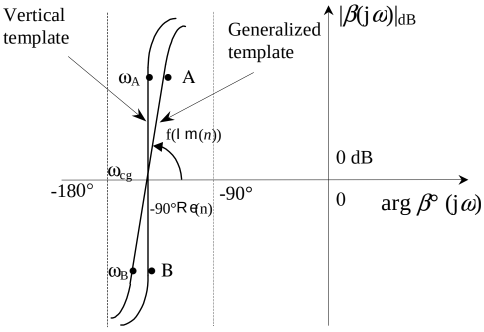

Fig.1. Representation of the vertical template and of the generalized template in the Nichols plane

II. Isodamping contours

In the time domain, the dynamic performances can be characterized by the first overshoot and the damping ratio of a step response. In order to guaranty these performances by using a frequency domain control methodology, it is necessary to have an equivalent of these dynamic performances in the frequency domain. The well-known magnitude contour in the Nichols plane can be considered as an iso-overshoot contour [4]. For the damping ratio, A. Oustaloup has constructed and defined a set of contours called "iso-damping" contours whose graduations are the damping ratios in the Nichols plane [3]. These contours have been constructed using an envelope technique. The contour is then defined as the envelope tangented by a set of segments (Fig.2). In the Nichols plane, each segment of the set can be considered as the rectilinear part of an open-loop Nichols locus that ensures the closed-loop damping ratio corresponding to the contour. This rectilinear part around gain crossover frequency, ω_{cg}, is the "generalized template" defined above.

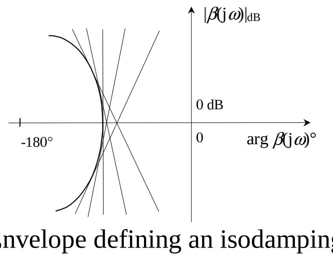

Fig.2. Envelope defining an isodamping contour in the Nichols plane

Isodamping contours can be defined analytically using a polynomial equation determined by interpolation of graphical data of each contour [3]. A contour Γ_ζ is thus defined by:

$$\Gamma_\zeta = \left\{ M(X,Y) \in P,\ X - \sum_{j=0}^{2} f_j(\zeta) Y^{2j} . = 0 \right\} \qquad (3)$$

with $$f_j(\zeta) = \sum_{k=0}^{3} a_{jk} \zeta^k , \qquad (4)$$

X and Y being the coordinates expressed in degrees and in decibels and a_{jk} the coefficients given in table 1.

The equation of the tangent to Γ_ζ at point (X_i, Y_i) is deduced from relation (3) and can be written:

$$Y = \alpha_2 X + \beta_2 , \qquad (5)$$

with $$\alpha_2 = \frac{1}{2Y_i \left(\sum_{k=0}^{3} a_{1k} \zeta^k \right) + 4Y_i^3 \left(\sum_{k=0}^{3} a_{2k} \zeta^k \right)} \qquad (6)$$

and $$\beta_2 = Y_i - \frac{1}{2Y_i \left(\sum_{k=0}^{3} a_{1k} \zeta^k \right) + 4Y_i^3 \left(\sum_{k=0}^{3} a_{2k} \zeta^k \right)} X_i . \qquad (7)$$

j/ *k*	0	1	2	3
0	-180.36	117.7	-74.316	40.376
1	-1.1538	3.8888	-5.2999	2.5417
2	-0.0057101	0.0080962	-0.0060354	0.0016158

Table 1. Values of coefficients a_{jk}

III. CRONE control

CRONE (the French acronym of "Commande Robuste d'Ordre Non Entier") control system design [5,6,7] is a frequency-domain based methodology using complex fractional integration. It permits the robust control of perturbed linear plants using the common unity feedback configuration. It consists on determining the nominal and optimal open-loop transfer function that guaranties the required specifications. This methodology uses fractional derivative orders (real or complex) as high level parameters that make easy the design and optimization of the control-system. While taking into account the plant right half-plane zeros and poles, the controller is then obtained from the ratio of the open-loop frequency response to the nominal plant frequency response. Three Crone control generations have been developed, successively extending the application fields [8]. In this paper, the third generation will be applied to a lightly damped MIMO plant.

A. Open-loop transfer function

The open-loop transfer function (Fig.3) of the initial third generation Crone method is based on the generalized template described previously and takes into account:

- the accuracy specifications at low frequencies;
- the generalized template around frequency ω_{cg};
- the plant behavior at high frequencies in accordance with input sensitivity specifications for these frequencies.

For stable minimum-phase plants, this function is written:

$$\beta(s) = \beta_l(s) \beta_m(s) \beta_h(s) . \qquad (8)$$

- $\beta_m(s)$, based on complex non-integer integration, is the transfer function describing the band-limited generalized template [1]:

$$\beta_m(s) = K\left(\frac{1+\frac{s}{\omega_h}}{1+\frac{s}{\omega_l}}\right)^a \left[\mathrm{Re}_{/i}\left\{\left(\left[\frac{1+\left(\frac{\omega_{cg}}{\omega_l}\right)^2}{1+\left(\frac{\omega_{cg}}{\omega_h}\right)^2}\right]^{\frac{1}{2}}\left(\frac{1+\frac{s}{\omega_h}}{1+\frac{s}{\omega_l}}\right)\right)^{ib'}\right\}\right]^{-q'\,sign\,b'} , \qquad (9)$$

q' being the smallest integer such that b' verifies $|b'| < \min(|b_1|,|b_2|)$ with:

$$|b_1| = \pi / \left|\ln\left(\left(1+\left(\frac{\omega_{cg}}{\omega_l}\right)^2\right) / \left(1+\left(\frac{\omega_{cg}}{\omega_h}\right)^2\right)\right)\right| \qquad (10)$$

and $$|b_2| = \pi / \left|\ln\left[\left(\left(1+\left(\frac{\omega_{cg}}{\omega_l}\right)^2\right) / \left(1+\left(\frac{\omega_{cg}}{\omega_h}\right)^2\right)\left(\frac{\omega_l}{\omega_h}\right)^2\right)\right]\right|, \qquad (11)$$

and K being computed to get a gain of 0 dB at ω_{cg}.

- $\beta_l(s)$ is the transfer function of order n_l proportional-integrator, whose corner frequency equals the low corner frequency of $\beta_m(s)$, so that joining $\beta_l(s)$ and $\beta_m(s)$ does not introduce extra parameters. $\beta_l(s)$ is defined by:

$$\beta_l(s) = \left(1+\frac{\omega_l}{s}\right)^{n_l} . \qquad (12)$$

If n_{pl} is the order of asymptotic behavior of the plant in low frequency ($\omega \ll \omega_l$), order n_l is given by $n_l \geq 1$ if $n_{pl} = 0$, and $n_l \geq n_{pl}$ if $n_{pl} \geq 1$, with $n_l=1$ canceling the position error and $n_l=2$ canceling the velocity error.

- $\beta_h(s)$ is the transfer function of order n_h low-pass filter, whose corner frequency equals the high corner frequency of $\beta_m(s)$, so that joining $\beta_h(s)$ and $\beta_m(s)$ does not introduce extra parameters. $\beta_h(s)$ is defined by:

$$\beta_h(s) = 1/\left(1+\frac{s}{\omega_h}\right)^{n_h} . \qquad (13)$$

If n_{ph} is the order of asymptotic behavior of the plant in high frequency ($\omega \gg \omega_h$), order n_h is given by $n_h \geq n_{ph}$, with $n_h = n_{ph}$ ensuring invariability of the input sensitivity function with the frequency, and $n_h > n_{ph}$ ensuring decrease.

At frequency ω_r for which the tangency will be reached, the modulus and the argument of the open-loop frequency response are expressed respectively by:

$$|\beta(j\omega_r)|dB = Y_r , \qquad (14)$$

and $$\arg\beta°(j\omega_r) = \frac{180}{\pi}\left[n_l\left(\theta_{rl} - \frac{\pi}{2}\right) - n_h\theta_{rh} + a\left(\theta_{rh} - \theta_{rl}\right)\right] \qquad (15),$$

with $\theta_{rl} = \arctan\left(\frac{\omega_r}{\omega_l}\right)$ and $\theta_{rh} = \arctan\left(\frac{\omega_r}{\omega_h}\right)$. (16)

The equation of the tangent to the Nichols locus at this frequency is given by:

$$Y = \alpha_{BO}\left(X - X_{BO}\right), \qquad (17)$$

with:

$$\alpha_{BO} = \left.\frac{d|\beta(j\omega)|dB}{d\arg\beta°(j\omega)}\right|_{\omega=\omega_r} \quad \text{and} \quad X_{BO} = \arg\beta°(j\omega_r). \qquad (18)$$

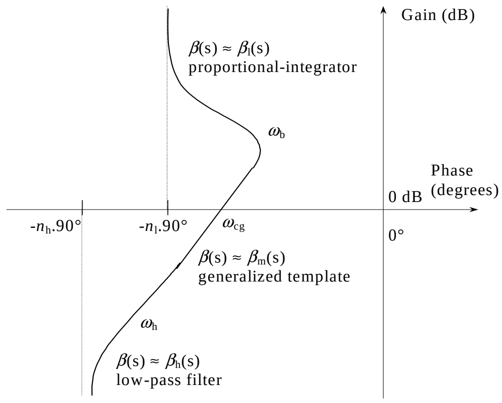

Fig.3. Different parts of the open-loop Nichols locus

B. CRONE methodology for SISO plants

The third generation CRONE methodology for SISO plants can be described in five points:

1 - You determine the nominal plant transfer function and the uncertainty domains. For a given frequency, an uncertainty domain (called "template" by the QFT users [9]) is the smallest hull including the possible frequency responses of the plant. The use of the edge of the domains makes it possible to take into account the uncertainty with the smallest number of data. To construct this domain securely, the simplest way is to define it convexly.

2 - You specify some parameters of the open-loop transfer function defined for the nominal state of the plant: the gain cross-over frequency and the rational orders n_l and n_h.

3 - You specify the bounds of the sensibility functions that you would like to obtain. Let $M_{r_{nom}}$ be the required resonant peak of the nominal complementary sensitivity function.

4 - Using the nominal plant locus and the uncertainty domains in the Nichols chart, you optimize the parameters a and b and the frequencies ω_l and ω_h in order to obtain the optimal open-loop Nichols locus. An open-loop Nichols locus is defined as optimal if it tangents (14) the $M_{r_{nom}}$ magnitude contour and if it minimizes the variations of M_r for the other parametric states. By minimizing the cost function $J = \left(M_{r\max} - M_{r\,nom}\right)^2$ where $M_{r_{\max}}$ is the maximal value of resonant peaks M_r, the optimal open-loop Nichols locus positions the uncertainty domains correctly, so that they overlap the low stability margin areas as little as possible (Figure 4: case (c) is the best configuration). The minimization of J is carried out under a set of shaping constraints on the four usual sensitivity functions.

5 - The last point is the synthesis of the controller. While taking into account the plant right half-plane zeros and poles, the controller is deduced by the frequency-domain system identification of the ratio of $\beta_{\mathrm{nom}}(\mathrm{j}\omega)$ to the nominal plant function transfer $G_{\mathrm{nom}}(\mathrm{j}\omega)$. The resulting controller $C(s)$ is a rational transfer function.

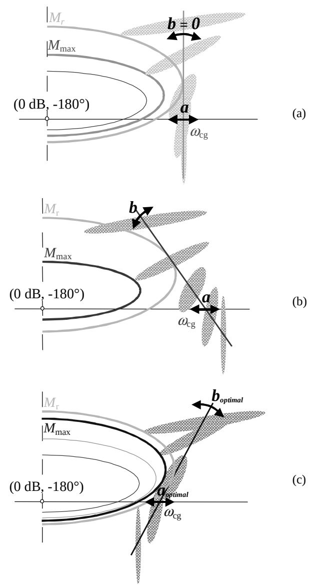

Fig.4. Optimal open-loop Nichols locus to position the uncertainty domains

C. CRONE methodology for MIMO plants

Principle:

The CRONE methodology for MIMO plants consists in finding a diagonal open-loop transfer matrix:

$$\boldsymbol{\beta}_0 = diag[\boldsymbol{\beta}_{0_i}], \qquad (19)$$

whose n elements are fractional order transfer functions.

It is parametered to satisfy the four following objectives:

- perfect decoupling for the nominal plant,
- accuracy specifications at low frequencies,
- required nominal stability margins of the closed loops (behaviors around the required cut-off frequencies),
- specifications on the n control efforts at high frequencies.

After an optimization of the diagonal open-loop transfer matrix , (19), the fractional controller is computed from the relation (20) and synthesized by frequency-domain identification.

$$C(s) = G_o^{-1}(s)\beta(s) \qquad (20)$$

Optimized solution

Let G_0 be the nominal plant transfer matrix such that $G_0(s)$=[$g_{ij}(s)$]$_{i,j\in N}$ and let $\boldsymbol{\beta}_0$ be:

$$\boldsymbol{\beta}_0 = G_0 K = diag\left[\boldsymbol{\beta}_{0_i}\right] = diag\left[\frac{n_i}{d_i}\right]_{i\in N}, \qquad (21)$$

where:

- $g_{ij}(s)$ is a strictly proper transfer function,
- $N=\{1,\ldots,n\}$,
- $\beta_{0_i} = \dfrac{n_i}{d_i}$ the element of the i_{th} column and row.

As mentioned above the aim of CRONE control for MIMO plants is to find a decoupling controller for the nominal plant. G_0 being not diagonal, the problem is to find a decoupling and stabilizing controller C [10]. This controller exists if and only if the following hypotheses are true:

$$- \; H_1 : [G_0(s)]^{-1} \text{ exist}, \qquad (22)$$

$$- \; H_2 : Z_+[G_0(s)] \cap P_+[G_0(s)] = 0, \qquad (23)$$

where $Z_+[G_0(s)]$ and $P_+[G_0(s)]$ indicate the positive real part zero and pole sets.

The controller $C(s)$ is:

$$C = G_0^{-1}\boldsymbol{\beta}_0 = \frac{adj(G_0)}{|G_0|}\, diag\left[\frac{n_i}{d_i}\right]_{i\in N}, \qquad (24)$$

with $adj(G_0(s))=[G_0^{ij}(s)]^{\mathrm{T}}=[G_0^{ji}(s)]$, $G_0^{ij}(s)$ being the cofactor corresponding to element $g_{ij}(s)$ and $|G_0|$ corresponding to determinant of $G_0(s)$.

Thus each term of the matrix C is written:

$$c_{ij} = \frac{G_0^{\,ji}}{|G_0|}\boldsymbol{\beta}_{0_i} \;\; \forall i, j \in N. \qquad (25)$$

The nominal sensitivity and the complementary sensitivity transfer function matrices are:

$$\mathrm{S}_0(s) = [I + \beta_0(s)]^{-1} = diag[S_{0i}(s)]_{1\le i\le n}, \qquad (26)$$

$$\mathrm{T}_0(s) = [I + \beta_0(s)]^{-1}\beta_0(s) = diag[T_{0i}(s)]_{1\le i\le n}, \qquad (27)$$

with

$$T_{0i}(s) = \frac{\beta_{0_i}(s)}{(1+\beta_{0_i}(s))}, \qquad (28)$$

$$S_{0i}(s) = \frac{1}{(1+\beta_{0_i}(s))}. \qquad (29)$$

For plants other than the nominal, the closed-loop transfer matrices $T(s)$ and $S(s)$ are no longer diagonal. Each diagonal element $T_{ii}(s)$ and $S_{ii}(s)$ could be interpreted as closed loop transfer functions coming from a scalar open-loop transfer function $\beta_{ii}(s)$ called equivalent open-loop transfer function:

$$\beta_{ii}(s)=\frac{T_{ii}(s)}{1-T_{ii}(s)}=\frac{1-S_{ii}(s)}{S_{ii}(s)}. \quad (30)$$

For each nominal open-loop $\beta_{0i}(s)$, many generalized templates can border the same required magnitude-contour or iso-damping contour in the Nichols plane. The optimal one minimizes the robustness cost function:

$$J=\sum_{i=1}^{n}\left(M_{\mathrm{p}_{\max_i}}-M_{\mathrm{p}_{\min_i}}\right)^2 \text{ or } J=\sum_{i=1}^{n}\left(\xi_{\max_i}-\xi_{\min_i}\right)^2, \quad (31)$$

where M_p is the resonant peak and ξ the damping ratio,

while respecting the following set of inequalities for $\omega\in$ R and $i, j\in N$:

$$\inf_G\left|T_{ij}(\mathrm{j}\omega)\right|\geq T_{ij_l}(\omega), \quad (32)$$

$$\sup_G\left|T_{ij}(\mathrm{j}\omega)\right|\leq T_{ij_u}(\omega), \quad (33)$$

$$\sup_G\left|S_{ij}(\mathrm{j}\omega)\right|\leq S_{ij_u}(\omega), \quad (34)$$

$$\sup_G\left|CS_{ij}(\boldsymbol{j}\omega)\right|\leq CS_{ij\,\boldsymbol{u}}(\omega), \quad (35)$$

$$\sup_G\left|SG_{ij}(\boldsymbol{j}\omega)\right|\leq SG_{ij\,\boldsymbol{u}}(\omega), \quad (36)$$

where G is the set of the plants.

As the uncertainties are taken into account by the least conservative method, a non-linear optimization method must be used to find the optimal values of the independent parameters of the fractional open-loop.

D. Extension to resonant plants

Some resonant frequencies must be included in the open-loop transfer function β_{0i} for the controller to be achievable and stable [11].
The first transfer matrix to consider is the input-disturbance sensitivity, T_0C^{-1}. Using:

$$T_0C^{-1}=S_0G_0=\left[\frac{d_i(s)\cdot g_{0_{ij}}(s)\cdot h_{ij}(s)}{d_i(s)+n_i(s)}\right] \quad (15)$$

this transfer function is resonant-free if

$$d_i(s)=\frac{\hat{d}_i(s)}{h_{ij}(s)} \;\; \forall j\in N. \quad (38)$$

The denominator of the i^{th} open-loop transfer function must satisfy all the following equations:

$$d_i(s)=\frac{\hat{d}_i(s)}{h_{i1}(s)}, d_i(s)=\frac{\hat{d}_i(s)}{h_{i2}(s)},\ldots, d_i(s)=\frac{\hat{d}_i(s)}{h_{in}(s)} \quad (39)$$

and therefore:

$$d_i(s)=\frac{\hat{d}_i(s)}{H_i(s)} \quad \forall i\in N, \quad (40)$$

where transfer functions $H_i(s)$ have in common the lightly damped modes of the ith row of G_0.

The second transfer matrix to consider is input sensitivity CS. Using:

$$C_0S=G_0^{-1}T=\left[\frac{p_{0_{ij}}(s)\cdot m_{ij}(s)\cdot n_j(s)}{d_j(s)+n_j(s)}\right], \quad (41)$$

this transfer function is resonant-free if

$$n_j(s)=\frac{n_j(s)}{m_{ij}(s)} \;\; \forall i\in N. \quad (42)$$

The numerator of the i^{th} open-loop transfer function must satisfy all the following equations:

$$n_j(s)=\frac{\hat{n}_j(s)}{m_{1j}(s)}, n_j(s)=\frac{\hat{n}_j(s)}{m_{2j}(s)},\ldots, n_j(s)=\frac{\hat{n}_i(s)}{m_{nj}(s)} \quad (43)$$

and therefore:

$$n_j(s)=\frac{\hat{n}_j(s)}{M_j(s)} \quad \forall j\in N, \quad (44)$$

where transfer functions $M_j(s)$ have in common some lightly damped modes of the jth column of G_0^{-1}.

Adding some lightly damped modes on the open-loop transfer functions causes resonant frequencies to appear on sensitivity and complementary sensitivity transfer functions. To attenuate their effect, transfer function $Q_j(s)$ is included in $\beta_{0i}(s)$ around each resonant frequency such that:

$$Q_j(s)=\left(\left(\frac{s}{\omega_j}\right)^2+2\xi\frac{s}{\omega_j}+1\right)\Big/\left(\left(\frac{s}{\omega_j'}\right)^2+2\xi'\frac{s}{\omega_j'}+1\right), \quad (45)$$

where:
- ω_j and ω_j' are frequencies close to the resonant frequency,
- ξ and ξ' are the damping factors.

IV. Robust control of a lightly damped plant with isodamping property

A. Description of the plant

The plant under study is an aircraft wing model (see figure 5). It is made of a beam and a tank. This structure has the same resonant frequencies as a real air wing. The problem is to control the vibrations which depend on the level of filling of the tank. Moreover, sloshing phenomena may appear, that makes the problem more complex. Two sets of piezoelectric ceramics are used as actuators in order to fight against bending and twisting vibrations. Two others piezoelectric ceramics are glued at the clamp of the beam to measure the vibrations and are used as sensors.
The characteristics of the plant are given in table 2.

	Beam	Actuator x 2
Length (mm)	1360	140
Width (mm)	160	75
Thickness (mm)	5	0.5
Density (kg/m^3)	2970	7800
Young Modulus (Gpa)	75	67
Piezoelectric Const. (pm/V)	-	-210
	Tank	
Ext. Diameter (mm)	110	
Int. Diameter (mm)	105	
Length (mm)	700	
x-location (mm)	1280	
Water Density (kg/m3)	1000	
Plastic Density (kg/m3)	1180	
Young Modulus (Gpa)	4.5	

Table 2. Plant characteristics

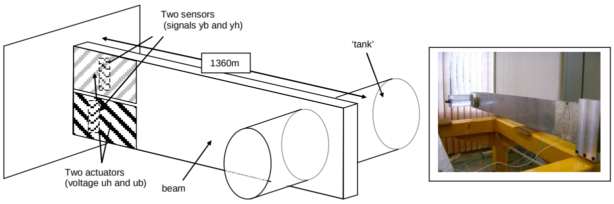

Fig.5. Model of the structure (beam with the tank)

In order to design the control system, the plant is described by a 2x2 MIMO model. The two inputs are the two actuators voltage and the two outputs are the sensors voltage. The first three modes are taken into account for the design of the control and thus the plant is described by the matrix of transfer functions given by:

$$G(s) = \begin{bmatrix} G_{11}(s) & G_{12}(s) \\ G_{21}(s) & G_{22}(s) \end{bmatrix} \text{ with} \qquad (46)$$

$$G_{11}(s) = \frac{k_{111}}{\frac{s^2}{\omega_{111}^2} + 2\frac{\varepsilon_{111}}{\omega_{111}}s + 1} + \frac{k_{112}}{\frac{s^2}{\omega_{112}^2} + 2\frac{\varepsilon_{112}}{\omega_{112}}s + 1} + \frac{k_{113}}{\frac{s^2}{\omega_{113}^2} + 2\frac{\varepsilon_{113}}{\omega_{113}}s + 1} + R_{11}$$

$$G_{12}(s) = \frac{k_{121}}{\frac{s^2}{\omega_{121}^2} + 2\frac{\varepsilon_{121}}{\omega_{121}}s + 1} + \frac{k_{122}}{\frac{s^2}{\omega_{122}^2} + 2\frac{\varepsilon_{122}}{\omega_{122}}s + 1} - \frac{k_{123}}{\frac{s^2}{\omega_{123}^2} + 2\frac{\varepsilon_{123}}{\omega_{123}}s + 1} + R_{12}$$

$$G_{21}(s) = \frac{k_{211}}{\frac{s^2}{\omega_{211}^2} + 2\frac{\varepsilon_{211}}{\omega_{211}}s + 1} + \frac{k_{212}}{\frac{s^2}{\omega_{212}^2} + 2\frac{\varepsilon_{212}}{\omega_{212}}s + 1} - \frac{k_{213}}{\frac{s^2}{\omega_{213}^2} + 2\frac{\varepsilon_{213}}{\omega_{213}}s + 1} + R_{21}$$

$$G_{22}(s) = \frac{k_{221}}{\frac{s^2}{\omega_{221}^2} + 2\frac{\varepsilon_{221}}{\omega_{221}}s + 1} + \frac{k_{222}}{\frac{s^2}{\omega_{222}^2} + 2\frac{\varepsilon_{222}}{\omega_{222}}s + 1} + \frac{k_{223}}{\frac{s^2}{\omega_{223}^2} + 2\frac{\varepsilon_{223}}{\omega_{223}}s + 1} + R_{22}$$

and the numerical data of the following tables .

		Empty tank	**Half-full tank**	**Full tank**
1° mode of flexion	k_{111}	0,015	0,006	0,01
	ω_{111} (rad/s)	7,22	5,1	4,59
	ε_{111}	0,0061	0,0062	0,0045
2° mode of flexion	k_{112}	0,01	0,002	0,005
	ω_{112} (rad/s)	53,78	41,2	34,84
	ε_{112}	0,012	0,046	0,006
1° mode of twisting	k_{113}	0,01	0,005	0,001
	ω_{113} (rad/s)	134,5	96,6	21,6
	ε_{113}	0,012	0,01	0,015
static term	R_{11}	0,12	0,14	0,085

Table 3. Values for $G_{11}(s)$

		Empty tank	**Half-full tank**	**Full tank**
1° mode of flexion	k_{121}	0,032	0,004	0,015
	ω_{121} (rad/s)	7,22	5,1	4,59
	ε_{121}	0,0087	0,0039	0,0041
2° mode of flexion	k_{122}	0,008	0,002	0,004
	ω_{122} (rad/s)	53,78	41,2	34,84
	ε_{122}	0,01	0,0046	0,006
1° mode of twisting	k_{123}	0,004	0,0012	0,001
	ω_{123} (rad/s)	134,5	96,6	21,6
	ε_{123}	0,011	0,0032	0,007
static term	R_{12}	0,02	0,018	0,02

Table 4. Values for $G_{12}(s)$

		Empty tank	**Half-full tank**	**Full tank**
1° mode of flexion	k_{211}	0,014	0,005	0,03
	ω_{211} (rad/s)	7,22	5,1	4,59
	ε_{211}	0,0061	0,0039	0,0068
2° mode of flexion	k_{212}	0,0065	0,002	0,004
	ω_{212} (rad/s)	53,78	41,2	34,84
	ε_{212}	0,012	0,0046	0,0069
1° mode of twisting	k_{213}	0,004	0,001	0
	ω_{213} (rad/s)	134,5	96,6	21,6
	ε_{213}	0,012	0,0039	x
static term	R_{21}	0,015	0,012	0,085

Table 5. Values for $G_{21}(s)$

		Empty tank	**Half-full tank**	**Full tank**
1° mode of flexion	k_{221}	0,02	0,004	0,007
	ω_{221} (rad/s)	7,22	5,1	4,59
	ε_{221}	0,0087	0,0052	0,0034
2° mode of flexion	k_{222}	0,009	0,0022	0,005
	ω_{222} (rad/s)	53,78	41,2	34,84
	ε_{222}	0,0129	0,0046	0,0056
1° mode of twisting	k_{223}	0,006	0,0011	0,03
	ω_{223} (rad/s)	134,5	96,6	21,6
	ε_{223}	0,0126	0,0026	0,067
static term	R_{22}	0,1	0,1	0,085

Table 6. Values for $G_{22}(s)$

B. CRONE control

The plant being a 2x2 MIMO system, the open-loop transfer function matrix is written as:

$$\beta(s) = \begin{bmatrix} \beta_{01}(s) & 0 \\ 0 & \beta_{02}(s) \end{bmatrix} \qquad (47)$$

whose two diagonal terms are defined by CRONE open-loop transfer functions of third generation (equ. 8).

The nominal plant corresponds to the empty tank. The objectives are to increase the damping ratio of the closed-loop plant such as to obtain a value of 0.1 and to guaranty the iso-damping property for the plant whatever the filling of the tank. So the iso-damping contour that each open-loop transfer function should tangent is of value 0.1. For each of the open-loop transfer function, the following configuration has been chosen:

- gain cross-over frequency equal to 3 rad/s,
- order n_l=-1 in order to limit the gain of the controllers in low frequencies and order n_h = 4 in order to limit the amplification of the noise in high frequencies,
- minimum of the complementary sensibility function *T* for the frequencies below the gain-cross over frequency:-5dB,
- maximum of the function *CS*: 50dB.

Let's now take into account the lightly damped modes of the plant. There are no lightly damped modes on the rows of the plant but there are some lightly damped modes in the columns of the inverse matrix of the plant coming from the determinant of the matrix since:

$$[G(s)]^{-1} = \frac{Com^t(G)}{\det(G)} \qquad (48)$$

Therefore, it is necessary to introduce in the open-loop transfer functions β_{01}(s) and β_{02}(s) the resonances of the modes at 7,09 rad/s, 8,12 rad/s and 57,11 rad/s.

Finally, a filter has been added in the open-loop transfer functions. It aims at shaping the open-loop Nichols locus by decreasing the gain and increasing the phase locally around the first resonance so that the uncertainties domains do not penetrate in the contours. The expression of the filter is the same for the two open-loop transfer functions and is written:

$$\beta_r(s) = \frac{\frac{s^2}{7^2} + 0.2\frac{s}{7} + 1}{\frac{s^2}{9^2} + 2\frac{s}{9} + 1} \qquad (49)$$

The results of the optimisation lead to the following optimal parameters:

- For β_{01}(s): a=0.0037, b'=3.05 ; q'= 5 ; Y_t = 0.4dB; ω_l=1.4 rad/s ; ω_h=3.3 rad/s ,
- For β_{02}(s): a=2.99, b'=1.81 ; q'= 5 ; Y_t = 0.71dB; ω_l=1.3 rad/s ; ω_h=3.3 rad/s ,

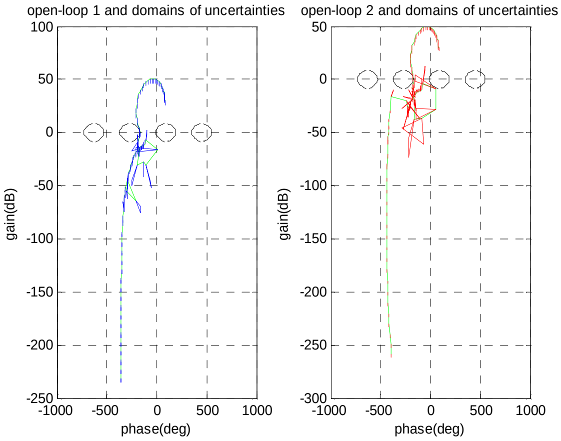

Fig.6. Nichols loci for β_{01}(s) and β_{02}(s)

The Nichols loci with the uncertainties domains are given in the Figure 6 for the two open-loop transfer functions β_{01}(s) and β_{02}(s).

The matrix of the controller is computed from the relation:

$$C(s) = G_0^{-1}(s)\beta(s) = \begin{bmatrix} C_{11}(s) & C_{12}(s) \\ C_{21}(s) & C_{22}(s) \end{bmatrix}. \qquad (50)$$

The four terms of this matrix are synthesized by identification in the frequency domain and the Bode diagrams are given in the figure 7.

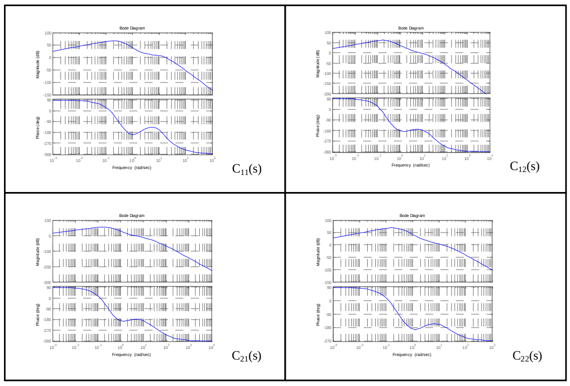

Fig.7. Bode diagrams of the terms of the controller

C. Results

The figure 8 shows the free response to a perturbation if there is no control and in the case of an empty tank. This figure gives the signal from the two sensors. It shows that it takes more than 200s to go back to balance.

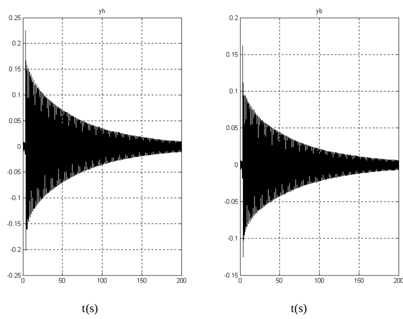

Fig.8. Response to a perturbation without control

The figure 9 shows the response to the same perturbation as previously with the CRONE controller and in three cases (empty tank, half-full tank and full tank). This figure gives the signal from the two sensors and the voltage of the two actuators.

Several observations can be drawn from these graphs:

- The voltages of the actuators are on their maximum level, even in saturation for the first oscillations since the D-Space card will limit the values of u_h and u_b at 1V (which corresponds to 130V on the actuator).
- It takes now less than 25s to go back to balance.
- The CRONE controller guaranties the robustness of the damping ratio of the response. The table 7 gives the value of this ratio for the three cases and the two sensors.

	Sensor yh	Sensor yb
Empty tank	0,11	0,11
Half-full tank	0,1	0,1
Full tank	0,12	0,12

Table 7. Values of the damping ratio for the 3 configurations of the tank with the CRONE controller

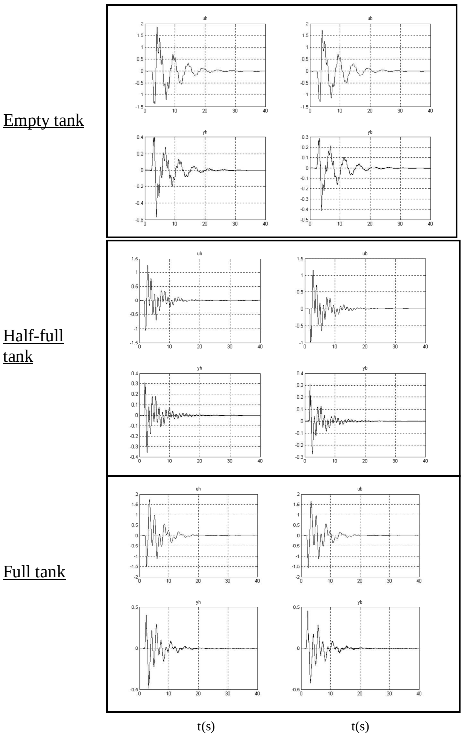

Fig.9. Response to a perturbation with the CRONE control

In order to evaluate the efficiency of the CRONE control; these results are compared with two others methodologies (LQR and GPC) whose results coming from [12] are given in the figure 10 and in the table 8. The CRONE controller is more robust while ensuring a better damping ratio.

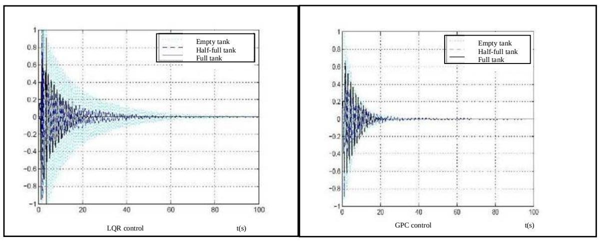

Fig.10. Response to a perturbation with LQR control and GPC control

	LQR controller	GPC controller
Empty tank	0.01	0.038
Half-full tank	0.03	0.04
Full tank	0.04	0.05

Table 8. Values of the damping ratio for the 3 configurations of the tank with LQR and GPC controllers

Conclusion

This article presents fractional robust control with iso-damping property. The plant under study is an aircraft wing model with a water tank. It is a multivariable plant with lighted damped modes. The proposed methodology is CRONE control. Results show that the vibrations are better damped with the CRONE control and that the time to go back to balance is divided by a factor 10. The tests on the plant with various levels of filling of the tank made it possible to highlight the properties of robustness of the damping ratio. The use of multivariable CRONE methodology and of iso-damping contours to carry out the control of a flexible structure with iso-damping property is thus clearly relevant.

References

[1] C. YQ, KL Moore (2005) Relay feedback tuning of robust PID controllers with isodamping property, IEEE Trans. on systems, Man and Cybernetics, partB-Cybernetics 35 (1), p23-31, Feb.

[2] S.G. Samko, A.A. Kilbas and O.I. Marichev,(1993) Fractional integrals and derivatives, *Gordon and Breach Science Publishers*

[3] A. Oustaloup, B. Mathieu, P. Lanusse (1995), Intégration non entière complexe et contours d'isoamortissement, *APII.* Vol.29 – n°2

[4] A.Oustaloup, V.Pommier, P.Lanusse (2003), Design of a fractional control using performance contours. Application to an electromechanical system, Fractional Calculus and Applied Analysis, Vol.6, Number 1

[5] A. Oustaloup, J. Sabatier and P. Lanusse (1999), From fractal robustness to the CRONE Control, Fractional Calculus and Applied Analysis, An international Journal for Theory and Applications, Vol. 2, pp. 1-30

[6] A. Oustaloup and B. Mathieu (1999). La commande Crone: du scalaire au multivariable, *Ed. Hermes*, Paris.

[7] A.Oustaloup, et al, (2000) The CRONE toolbox for Matlab, 11th IEEE International Symp. on Computer-Aided Control System Design, CACSD - Anchorage, Alaska, USA, September 25-27

[8] A. Oustaloup, B. Mathieu and P. Lanusse (1995), "The CRONE control of resonant plants: application to a flexible transmission", European Journal of Control, Vol. 1, pp. 113-121.

[9] I.M. Horowitz (199'), Quantitative feedback design theory - QFT, QFT Publications, Boulder, Colorado

[10]A. I. G Vardulkis (1987), Internal stabilization and decoupling in linear multivariable systems by unity output feedback compensation, IEEE Trans. on Autom. Control, August 32

[11]D. Nelson Gruel, P. Lanusse, A. Oustaloup, V. Pommier (2007), Robust control system design for multivariable plants with lightly damped modes, ASME conference, IDETC/CIE, Las Vegas, USA, Sept. 4-7

[12 J. Richelot (2006), « Contrôle actif des structures flexibles par commande prédictive généralisée », Thèse de l'Université Paul Sabatier Toulouse I